On the structure and control of near wall turbulence

Javier Jiménez
School of Aeronautics, Universidad Politécnica, 28040 Madrid, Spain and Center for Turbulence Research, Stanford University, Stanford, California 94305

(Received 9 March 1993; accepted 17 August 1993)

A simplified self-sustaining cycle is proposed for the events in the near wall region of a turbulent boundary layer. An approximate quantitative analysis of the resulting model predicts the right dimensions for the sublayer streaks and for other flow structures. The model is checked further by applying it to a set of numerical simulations in which the longitudinal and transverse no-slip conditions are applied at different positions with respect to the wall, and to the analysis of flow over riblets. Substantial changes in the flow statistics are obtained, including drag reductions, and the resulting trends are also predicted correctly by the model.

I. INTRODUCTION

Turbulent flow near walls is of sufficient theoretical and practical importance that it has always been in the mainstream of turbulence research.[1] It is still not completely understood, but the last decade has seen important advances, due both to the introduction of new experimental techniques and to the appearance of computers of sufficient power for realistic simulations of simple wall bounded flows.[2] This improved understanding has led to the realization that these flows can be controlled and to the introduction of practical devices, which are able to improve the drag characteristics of boundary layers in some circumstances.[3,4,5] This, in turn, has opened new opportunities for the theoretical study of the basic mechanisms of wall bounded turbulence and has renewed the interest in its final elucidation.

We restrict ourselves in this paper to the near wall region in flows subject to little or no pressure gradient. We define our region of interest as that lying between the wall and the inner end of the logarithmic profile. It is known that this is the seat of the largest rate of turbulent energy production and also a place where viscosity interacts strongly with turbulence. We define our coordinate system as x, y, and z for the streamwise, normal and spanwise directions, and we use wall units based on the average spanwise vorticity at the wall Ω. The friction velocity is defined as usual as $u_\tau=(\nu\Omega)^{1/2}$, where ν is the kinematic viscosity and lengths are normalized as $l^+=lu_\tau/\nu$. Experimentally, the near wall region lies below $y^+\approx 50$.

This part of the flow is known to be dominated by quasistreamwise vortices, and by alternating streamwise streaks of high and low velocity.[6,7] The kinematics of the vortical structures in this region have been reviewed recently in Ref. 8, and extensive statistical and structural information is available from numerical and experimental studies.[9–13] Still, there is no general consensus on the details of the flow dynamics.

In Sec. II we describe briefly a plausible conceptual model based on our interpretation of the results of the theoretical and experimental advances of the last few years. While most of the ideas in that section can be found elsewhere, they represent only a fraction of the alternatives proposed by different investigators, and the way that they are put together here is personal and should not be taken as the consensus view in the field. The rest of the paper is devoted to exploring and validating the quantitative consequences of our interpretation. Some of them are discussed in Sec. III, where it is shown that they can explain the relative and absolute size of the various structures in the undisturbed wall region. At the end of that section we will also be ready to make explicit the nature of the dynamical assumptions underlying our model. In Sec. IV we present some numerical experiments designed to distinguish between this and some partially competing interpretations. In Sec. V we relate our numerical experiments to the problem of drag reduction by the use of riblets, and we show again that the our model is qualitatively and quantitatively consistent with the observed facts. Finally, our conclusions are summarized in the final section.

II. THE CONCEPTUAL MODEL

The main features of the flow in the near wall region can be seen in Fig. 1, which corresponds to a low Reynolds number boundary layer. The figure displays two sets of vortex lines. Those in the first set are drawn through points along the edge of the periodic computational box at $y^+\approx 4$, and run approximately spanwise. At this level, very close to the wall, the dominant vorticity is always ω_z and is equivalent to an approximately uniform longitudinal shear. Still, some structure is present, in the form of roughly streamwise lanes along which the vortex lines bulge above the wall surface. Since vorticity is proportional to the local density of vortex lines, these lanes correspond to areas of low wall shear, and of low velocity at a given distance from the wall. They are the low-velocity streaks, as can be seen by the fluctuating velocity isolines on the vertical plane at the far end of the box.

The second set of vortex lines is drawn through a site of particularly intense ω_x near the right-hand side of the box, at $y^+\approx 50$. This is the upper edge of the wall region, as we have defined it here, and the vortex lines are seen to form part of a large hairpin that spans most of the thickness of the boundary layer. The legs of the hairpin extend back into the wall region, where they take the form of horizontal quasistreamwise ω_x vortices. From the position of the right-hand leg with respect to the central streak, it is

 1070-6631/94/6(2)/944/10/$6.00

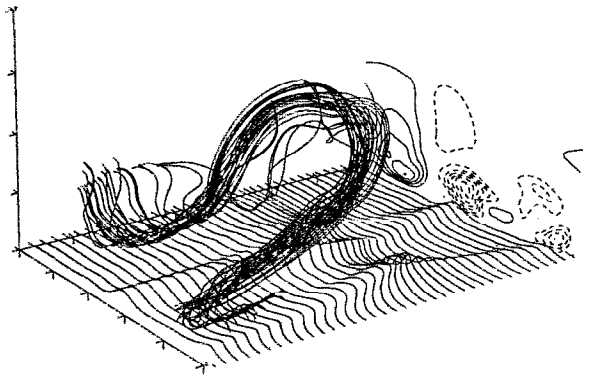

FIG. 1. Direct numerical simulation of a zero pressure gradient boundary layer.[40] Here $Re_\theta=250$. The numerical method is fully spectral[41] with modal resolution $36\times36\times97$; flow is periodic in $x^+\times z^+=300\times240$, going from left to right. The horizontal extent of the figure is a full computational box. Vortex lines are described in the text. Isolines are in the downstream boundary: u' increment: $\pm0.05U_\infty$; a dashed line is negative.

clear that the upwash from the hairpin is creating the vertical velocity that deforms the vortex lines away from the wall. This process, by which the quasistreamwise vortices pump low-velocity fluid away from the wall and high-velocity fluid close to it, has long been recognized as the basic process for the formation of the streaks.[7,14,15] In the particular case of Fig. 1 a second hairpin, not shown in the figure, less coherent and closer to the wall, exists toward the front of the box, staggered to the right of the one that is represented in the picture. Each of the two streaks is pumped by one leg of one of the hairpins and by the opposite leg of the other, although not at the same streamwise location. This is typical. It was shown in Ref. 15 that streaks tend to be flanked by vortices of opposite signs in a staggered arrangement, although at any given location, there is usually only one of them.[8,11] Figure 1, and many others in direct numerical simulation fields, suggest that this is implemented by sharing parts of different more or less complete hairpins vortices. Fully developed hairpins are flow features of the logarithmic and core regions[16] that scale on the thickness of the boundary layer, while streaks are near wall phenomena that scale on wall units. There can be no one-to-one correspondence between them. The streaks are associated with the almost horizontal legs, and are influenced little by the rest of the hairpin. In fact, on higher Reynolds number flows, many hairpins are asymmetric or incomplete and, by the time that they have evolved enough to have strong streamwise vortices as their legs, much of their heads have lost their identity into the general turbulence of the core flow.[8]

Because the streaks seem to be associated with the effect of almost streamwise vortices, their formation can be described almost two dimensionally in the cross-stream plane (y,z), and linearly, in the sense that the formation of the high and low streamwise velocity regions does not influence the behavior of the vortices themselves.[17] It is easy to see that, as long as all features in a flow are independent of x, there can be no effect of the streamwise flow into the transverse velocities. If $\partial/\partial x=0$, the equation for the transverse flow is incompressible, and the equation for the streamwise vorticity does not contain any contribution from the longitudinal velocity.

On the other hand, the transverse flow modifies the distribution of streamwise velocity, carrying low-velocity fluid into high-velocity regions, and vice versa. This process, which results in the formation of streaks aligned strictly to the mean flow, does not introduce any longitudinal gradients, and could continue forever in the absence of perturbations. In the end the whole velocity difference across the wall layer would be redistributed into alternating streaks of maximum and zero longitudinal velocity. Because of the logarithmic nature of the velocity profile in the outer region of the boundary layer, the velocity difference across the wall layer is essentially the same as across the whole boundary layer.

One consequence of the two-dimensionality is that this process alone cannot explain the maintenance of wall turbulence. Even if streamwise vortices are introduced by the initial conditions, they cannot draw energy from the mean flow, and eventually decay viscously. On the other hand, once the presence of streamwise vortices is assumed, their effect on the streaks explains much of the dynamics of the wall region. The advection of longitudinal momentum by the transverse velocities carries energy from the mean flow into turbulent, u', fluctuations and generates net Reynolds stresses that eventually deform the mean velocity profiles. In the presence of a wall, the high-velocity fluid carried by the vortices to the neighborhood of the wall forms thin viscous layers, which increase locally the wall friction. Even if the same effect generates other areas of low friction, it can be shown that the net effect is an increase of the total drag, which is roughly of the right magnitude to explain the higher friction drag of turbulent layers.[17,14]

The cycle has to be closed by some mechanism for the regeneration of the streamwise vortices. There is evidence from numerical experiments that this is preceded by the formation of thin horizontal layers of streamwise vorticity, which appear at the edge of the viscous sublayer.[15] These layers roll up into discrete cores that concentrate most of their vorticity, in a process that is also two dimensional in the (y,z) plane, and which is driven by the interaction of the vorticity in the layer with the zero normal velocity condition at the wall.[18] In this process there is some viscous generation of secondary streamwise vorticity of opposite sign at the wall, which is ejected into the flow and which can form new structures,[19,20] but, as in any essentially two-dimensional process, no energy flows from the mean into the transverse flow.

The formation of the horizontal vortex sheets has to be initiated by some process that breaks the uniformity in x. There are plenty of three-dimensional perturbations in a turbulent boundary layer, including all the large-scale "inactive" (u,w), motions coming from the core flow. These would distort the streaks, even if they were formed in a strictly two-dimensional fashion, and could seed any subsequent flow evolution. In fact, the streaks in Fig. 1 are seen to be distorted, in this case most probably by the effect

of the hairpin head passing above them. It was observed in Ref. 11 that, right before the violent events that culminate in the formation of new streaks, the old streak develops a transverse undulation that "breaks" at the climax of the event. In that case, the trigger for the undulation was also identified as a separate quasistreamwise vortex passing overhead. The importance of the lateral displacement of the streaks on the regeneration of turbulence has also been recognized theoretically and experimentally by other investigators.[6,21,22]

Of all the perturbations coming from the core flow, some will be more amplified than others by the instabilities of the velocity gradients present near the wall, and those most amplified will eventually dominate the dynamics. The gradients most likely to become unstable are the thin longitudinal walls of ω_y vorticity that separate laterally the high- from the low-velocity streaks.[23] They are basically vertical shear layers whose natural Kelvin–Helmholtz instability will tend to amplify their lateral undulations.

The perturbations, amplified by the lateral instability of the shear layers, introduce a longitudinal gradient that interacts with the average shear and injects energy into the transverse flow. It has been noted often that this interaction is "fast," in the sense that the perturbed ω_y is sheared in a time that is short compared to the one needed for its self-interaction, and the rapid distortion theory for sheared turbulence has been studied on several occasions in the context of wall turbulence.[21,24–26] Because there is no time for nonlinear interactions of the flow with itself, the process is linear and can be treated analytically.

As the total shear $S=\Omega t$ increases, the longitudinal u' component is amplified the fastest, the spanwise w is amplified more slowly, and the vertical velocity v is damped. At the same time, the longitudinal integral scale increases, while the transverse z scale stays essentially unchanged, and the normal y scale decreases, especially for the transverse w component.[27]

The lengthening of the longitudinal scale shows that the flow is becoming two dimensional in the cross plane, while the selective amplification of the u component reflects the formation of the streaks by the action of the longitudinal vorticity on the mean shear. Considering now the resulting flow in the transverse plane, the combination of a large horizontal velocity component with a small vertical one, plus a length scale that is much smaller in y than in z defines the formation of horizontal vortex sheets. In essence, the ω_y component of the initial perturbation is tilted forward into ω_x and squashed into the form of sheets parallel to the wall, while the dominant ω_z is rotated by the streamwise perturbations into new ω_y that defines the borders of new streaks.

Some representative dimensions might be of interest at this point. The average distance between neighboring streaks is[28] $z^+\approx 100$, relatively independent of Reynolds number, and it has been shown[11] that turbulence decays when streaks are forced to be narrower than that. The streamwise vortices have radii $R^+\approx 10$–15, also independent of Reynolds number, at least in the range $\mathrm{Re}_\tau<200$, for which they have been measured.[8,9,29] The vorticity layers from which they form have thickness $\delta^+\approx 5$–10, and stand at about that same distance from the wall.[15] This is also the distance away from the wall of the bottom of the streamwise vortices.[9] The streamwise length of the streaks is much larger, of the order of $x^+\approx 1000$.

Not all the structures in the wall region scale in wall units independently of Reynolds number. There is evidence that the circulation of the streamwise vortices, γ/ν, increases slowly with Reynolds number,[29] and so does the peak intensities of the two transverse velocity fluctuations, v' and w', as well as the maximum Reynolds stress.[13] These two trends can be related if it is assumed that the transverse flow is dominated by the streamwise vortices. In contrast, the longitudinal fluctuations u' scale well in wall units, in agreement with the idea that the streak formation saturates only when the full velocity difference across the wall layer has been brought down to the viscous scale, independent of the strength of the streamwise vortices.

The reason for the dependence of the vortex intensity on the bulk Reynolds number is not clear, and bears on the question of the relationship between the wall region and the outer flow. It has been suggested that it is due to increased stretching of the vortices,[13] but this explanation contradicts the observed constancy of the radii. We suggest that a more likely explanation is that the perturbations initiating the lateral undulations of the streaks are larger at higher Reynolds number, since they are generated by the core flow, and should increase with U_∞/u_τ. Larger perturbations would result in deeper waves, which would inject more vorticity into the resulting vortex layers. We know, however, of no quantitative way of checking this hypothesis.

III. THE SIZE OF THE STREAKS

The conceptual model in the previous section can be used to obtain a rough estimate of the size of the different structures in the wall region, which can then be checked against the experimental evidence.

Let us begin with a flow dominated by streaks separated by an average distance $\Delta z=W$. As long as there is no velocity variation with x there can be no interaction between the streaks and the mean flow, but, as soon as some perturbation appears, it is tilted by the shear into an elongated structure, which has the same lateral extent as the initial perturbation, but which is compressed in y by the tilting. Assume that the streak behaves like two adjacent planar jets, one moving forward and one backward, each of which has a width $W/2$. The most amplified mode in a planar jet is sinuous, with a wavelength 2.5 times larger than the width of the jet,[30]

$$L\approx 5W/4. \tag{1}$$

Let us now estimate the thickness of the horizontal vortex sheets resulting from the distortion of this perturbation. The essence of the process is contained in the evolution of a vertical slab of ω_y vorticity whose thickness is $L/2$, initially parallel to the cross (y,z) plane, and which is tilted by the mean shear Ω.

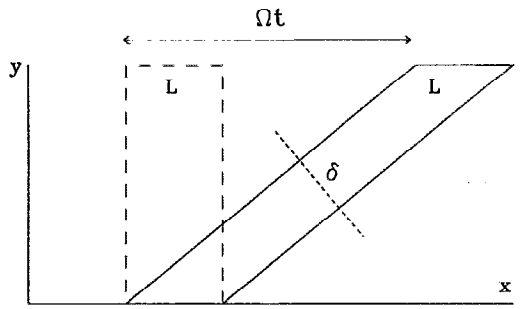

FIG. 2. Schematic representation of the tilting of a vertical blob of ω_y into a thin sheet of quasihorizontal vorticity.

After a time $t \gg \Omega^{-1}$, it will form with the wall an angle $\tan^{-1}(1/\Omega t) \approx 1/\Omega t$, and its vorticity, which is always approximately aligned parallel to the sheet, will be subject to an effective strain that is equal to the projection of the shear on the plane of the structure. Points of the sheet located at equal distances from the wall move at the same velocity, and the horizontal extent of the sheet remains always equal to $L/2$, but its normal thickness decreases proportionally to its tilting angle as (Fig. 2)

$$\delta = L/2\Omega t. \tag{2}$$

The evolution is approximately equivalent to that of a horizontal vorticity layer being stretched by an axial strain $u=\beta x$, where $\beta = -(1/\delta)d\delta/dt = 1/t$. The full equation for the axial vorticity (now approximately streamwise) is

$$\frac{\partial \omega_x}{\partial t} - \frac{y}{t}\frac{\partial \omega_x}{\partial y} = \frac{\omega_x}{t} + \nu \frac{\partial^2 \omega_x}{\partial y^2}, \tag{3}$$

which has a similarity solution of the form

$$\omega_x \sim t^{-1/2} \exp(-3y^2/4\nu t). \tag{4}$$

This is a long time limit in which a Burger's vortex sheet, subject to weak axial strain, expands under the action of viscosity as $\delta \approx 2(\nu t)^{1/2}$. The short time behavior is the contraction given by Eq. (2), and both trends intersect at $t_m \approx (L^2/16\Omega^2\nu)^{1/3}$, at which time the vorticity is maximum and the thickness of the layer reaches a minimum,

$$\delta_m \approx (2L\nu/\Omega)^{1/3} \approx (5W\nu/2\Omega)^{1/3}. \tag{5a}$$

Expressed in wall units based on Ω,

$$\delta_m^+ \approx (5W^+/2)^{1/3}. \tag{5b}$$

It is at this stage that layers of streamwise vorticity would be identified experimentally as such. Note that, if the initial perturbation consisted of alternating transverse layers of high and low ω_y, the shear would tilt them into alternating horizontal layers of high and low ω_x, and δ_m would stand as much for the thickness of the layers as for their standoff distance away from the wall.

The ω_x layer formed in this way rolls eventually into streamwise vortices, whose size can be estimated by equating the area in the sheets to that in the cores. Each streak will generate on the average two vortices of opposite sign, each of them with an area $W\delta_m/2$ and radius

$$R^+ \approx (W^+\delta_m^+/2\pi)^{1/2} \approx \delta_m^{+2}/\sqrt{2\pi}. \tag{6}$$

These vortices act on the transverse flow approximately as point vortices located at a distance $h^+ = R^+ + \delta_m^+$ from the wall. The effect of such a vortex is to create a transverse recirculation bubble[14] whose height is $2h^+$, and whose width at the wall is $2\sqrt{3}h^+$. We now close our estimate by claiming that an average streak contains two vortices of opposite sign, at least when averaged along its length, and that the distance between adjacent streaks is the width of the two recirculation bubbles,

$$W^+ \approx 4\sqrt{3}h^+ \approx 4\sqrt{3}(R^+ + \delta_m^+). \tag{7}$$

The argument is that narrower streaks, containing two vortices that are closer together than the width of their bubbles, do not subsist for long times because the vortices pair, while wider ones, initially formed by vortices that are so far from each other so as not to interact, split eventually as each vortex creates its own streak by acting on the mean shear.

Equations (5b), (6), and (7) can now be combined into a single one for the standoff distance,

$$\frac{1}{10\sqrt{3}}\delta_m^{+3} - \frac{1}{\sqrt{5\pi}}\delta_m^{+2} - \delta_m^+ = 0, \tag{8}$$

whose relevant root is $\delta_m^+ \approx 6.9$. The resulting vortex radius and streak width are $R^+ \approx 12$ and $W^+ \approx 130$. All these estimates are in the range of values observed experimentally.

It should be stressed at this point that we do not claim that the foregoing is a rigorous derivation of the width of a streak, and that much of the numerical agreement with the experiment is probably fortuitous. The arguments presented here are only order of magnitude considerations and they should be taken as such. We do, however, claim that the different mechanisms proposed for the life cycle of the streak have dynamical significance, and that the approximately correct ratio of the different dimensions in the resulting model shows that it captures their relative importance within the cycle.

In summary, the dynamical assumptions that were used in the estimates were the following: first, that the streamwise scale of the perturbations is selected by the streaks as a fixed multiple of its spanwise width; second, that this perturbation is converted by the mean shear into a vortex sheet of streamwise vorticity whose thickness and standoff distance are determined by an equilibrium between the tilting and the viscous diffusion; and last, that the sheets roll into streamwise vortices, whose distance from the wall determines the width of a new streak.

Several drastic simplifications are embedded in this analysis. The first one is that the mean shear stays constant while the tilting process takes place. This is the linear assumption implicit in rapid distortion theory and is discussed extensively in Ref. 25. A second simplification is that the sheets reach their minimum thickness and then decouple from the shear to behave like essentially unstrained. This is an order of magnitude approximation. As long as the sheets form an appreciable angle with the wall

the tilting is too fast for them to decouple. It is only after they become almost horizontal that the tilting process slows down and the decoupling becomes possible. It is also then that viscosity can become important. There is no guarantee that any particular perturbation will become strong enough to decouple and roll into a vortex. The assumption in our analysis is that weaker ones are eventually dissipated, and are of no importance to the maintenance of turbulence.

IV. A CONTROL EXPERIMENT

One of the most powerful techniques for investigating the structure of a flow is to study its response to perturbations. One of the main advantages of numerical simulations with respect to physical experiments is their ability to implement perturbations that are difficult to duplicate physically, but that can throw light on the mechanics of a particular phenomenon. As an added benefit, when a desirable effect is found in this way, a physical approximation can sometimes be devised to take advantage of it in practical situations. Above we have outlined a theoretical model for turbulence near walls, in which the key regeneration event is the rapid interaction of a mean streamwise shear with essentially random fluctuations introduced by the core flow and selected by the instability of the velocity gradients present near the wall.

This is not the only possible model. It is known that when a vortex approaches a viscous wall it sometimes produces a strong ejection of substantial quantities of secondary vorticity, resulting in the generation of a net Reynolds stress.[19,31] It has been suggested that this violent event, in which the longitudinal vortices interact with the viscous wall, is a model for the sublayer "bursts," and that it is responsible for most of the production of turbulent stresses in the near wall region and, ultimately, for the skin friction. A clear summary of this point of view is Ref. 20.

These two models are very different, but they are difficult to tell apart in natural boundary layers. The problem is that the key boundary condition is different in each case, but that both conditions are applied at the same point in the natural flow. The rapid distortion model depends on the presence of a no-slip condition for the longitudinal velocity u, which is responsible for the maintenance of the longitudinal shear. The transverse no-slip condition, $w(y=0)=0$, plays no role in this model, except as a damping agent for streamwise vortices that happen to come near the wall.

The viscous interaction model depends critically on the presence of the transverse no-slip condition. It is through it that the interaction is implemented, and eventually results in the bursting phenomenon and in the generation of Reynolds stresses.

It is therefore possible, in principle, to distinguish between the two models by removing selectively one of the two boundary conditions, and observing the results. This is difficult in natural layers, in which both no-slip conditions are either present or absent at the wall, but it can be done numerically. Indeed, in a preliminary numerical experiment in which the transverse condition at the wall was substituted by a free slip, $\partial w/\partial y=0$, the skin friction was observed to increase,[32,5] lending support to the inviscid model in which transverse viscous interactions are only dissipative. We extend this numerical experiment here, and make it quantitative.

The tool is a simulation code initially developed for feedback control of the skin friction in plane turbulent channels.[5] In one of its modes of operation it fixes the local transverse wall velocity as a fraction of the instantaneous velocity at a given height,

$$w(x,0,z)=\alpha w(x,h,z). \tag{9}$$

There are several important cases. Choosing $\alpha=0$ is equivalent to the natural no-slip condition. If h^+ is small and w can be taken to vary linearly near the wall, $\alpha=1$ is approximately equivalent to a transverse free slip boundary.[32] Under the same assumption, $\alpha<0$ is equivalent to a no-slip transverse condition applied at a "virtual transverse wall" located at $y=-\alpha h/(1-\alpha)$. When $\alpha\in(0,1)$, this approximate condition is applied at a point below the wall. In practice, the velocity does not vary linearly and the location of those approximate conditions has to be measured empirically. Note that, in all cases, the no-slip condition for the longitudinal velocity u is maintained unchanged at $y=0$.

Several experiments were run using this code with different values of α. In all the cases described here the test point was located at $h^+\approx 10$. A few other cases using different test heights were also run. Those using $h^+<10$ had roughly the same behavior as the ones described here, while those using greater test heights tended be less effective as controls. Since $h^+=10$ corresponds to the edge of the viscous sublayer, and is close to the position of the streamwise vortices, it is a natural boundary for any attempt to modify the turbulent structure near the wall. In essence, the flow underneath that location can be considered laminar, with only a few degrees of freedom, while above that level there are many more flow structures that have to be modified independently.

The experiments were run at a nominal $\mathrm{Re}_\tau\approx 120$, which varied between 100 and 160 as a consequence of the control. The computational domain was $4\pi\times 4\pi/3$ in x and z. The code is spectral, with a resolution of 32×32 Fourier modes in x,z, before dealiasing, and of 65 Chebyshev modes in y, which are not dealiased. This resolution is insufficient for structural work, especially at the highest Re_τ, but it should be enough to study the variations of the low-order statistics.[5] On the other hand, the relatively low resolution allowed us to do an extensive study of the effects of different boundary conditions.

The code was run long enough to reach a statistically steady flow, and mean and fluctuation profiles were compiled for the three velocity components and for the main Reynolds stress $\langle -u'v'\rangle$.

The profiles for the spanwise velocity fluctuation w', obtained for different values of α, are given in Fig. 3, where each profile is normalized with its own friction velocity. In those cases in which $\alpha<0$, the profiles show a clear minimum, which can be identified as the position of the "virtual

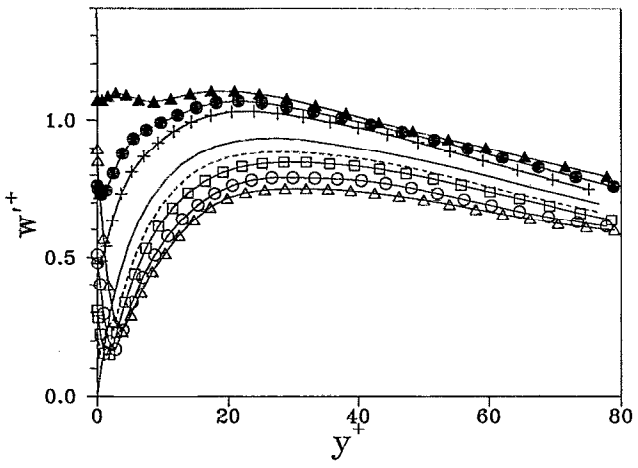

FIG. 3. Transverse turbulence intensity profiles for controlled channels with different α. Note the minimum in w', which is present in the profiles with $\alpha<0$. Open triangles: $\alpha=-2$, circles: -1, squares: -0.5, dashed line, -0.33, solid line: natural channel, crosses: 0.5, solid circles: 0.75, solid triangles: 1.

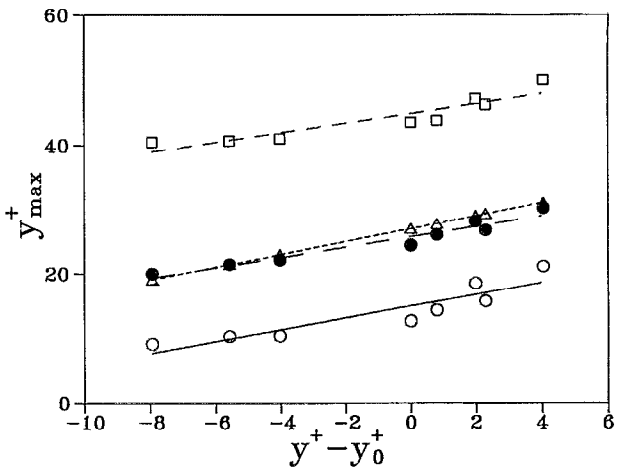

FIG. 5. Absolute position of the maxima of the fluctuation profiles as a function of the offset of the w' maximum with respect to the natural channel. From now on, this offset will be used as a measure of the offset of the transverse profile. ○: u', regression slope 0.91; □: v', slope 0.74; △: w', slope 1.0; ●: $\langle -u'v' \rangle$, slope 0.81.

wall" at which $w\approx 0$. The distance from that minimum to the real wall, where $u=0$, increases with the magnitude of α. In the cases in which $\alpha>0$, where, according to the previous discussion, the virtual transverse boundary is below the longitudinal one, the minimum is either absent or much weaker.

As the location of the minimum varies, so does the position of the maximum of w', which gets farther away from the wall as α becomes more negative. Figure 4 displays the displacement of the location of the maxima and of the minima of w' with respect to those of the natural channel, for those cases in which both can be identified ($\alpha<0$). It can be seen that the distance between them remains constant, $\Delta y^+\approx 20$, and that the net effect is a translation of the w' profile as a whole, without a change in its thickness. Since w in the wall layer is due primarily to the streamwise vortices, it is tempting to identify this translation as a drift of the vortices away from the wall, in response to the offset between the $w=0$ and $u=0$ boundary conditions. Since the location of the maximum is easier to measure than that of the minimum, and since it can also be defined for those cases in which $\alpha>0$, in which the minimum does not exist, we will use it from now on as a measure of the vertical displacement of the transverse flow in response to the perturbation.

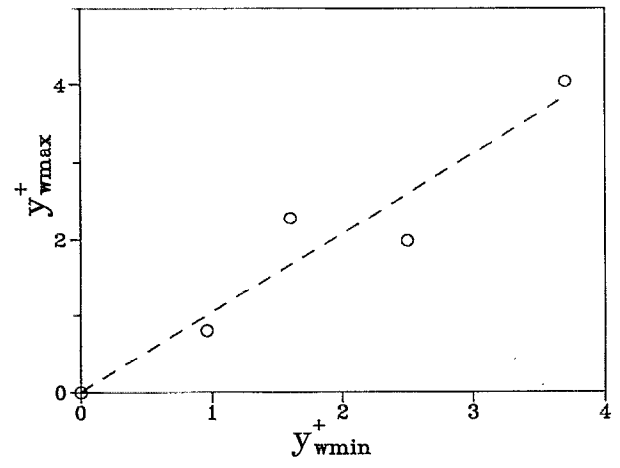

FIG. 4. Displacement of the position of the maximum of w' with respect to the natural channel, as a function of the position of the minimum of w' above the wall. The regression line has a slope of 1.04. Each flow is normalized with its own friction velocity.

The variation of the location of the maxima of all the fluctuation profiles as a function of the transverse offset is shown in Fig. 5. In all cases, except possibly for v', the slope of a linear regression line is consistent with a rigid translation of the whole flow pattern as a consequence of the drift of the vortices. The case of the maximum v', in which the drift seems to be slower ($dy_v^+/dy_w^+\approx 0.74$), is complicated by the fact that it is also the one farthest away from the wall and that it is probably influenced by conditions outside the wall layer. It is also the widest maximum and the hardest one to define.

As the maxima move away from the wall, their amplitude decreases slightly (Fig. 6), except for u', which stays approximately constant. This is true for quantities expressed in wall units, even if it will be seen later that the friction velocity itself becomes smaller as the transverse flow is pushed away from the wall. The decreasing trend would be somewhat more pronounced if expressed in absolute units. This behavior is inconsistent with a dynamical model in which the dominant phenomenon is the interaction of transverse velocity with the no-slip wall. In those cases in which no transverse wall can be defined (negative offsets), for which the interaction with the transverse wall is effectively being removed, the transverse flow not only does not decrease, but actually becomes strongest. This is even true in the limiting case $\alpha=1$, which is approximately equivalent to a free slip transverse condition for which the transverse viscous interaction is completely absent. On the

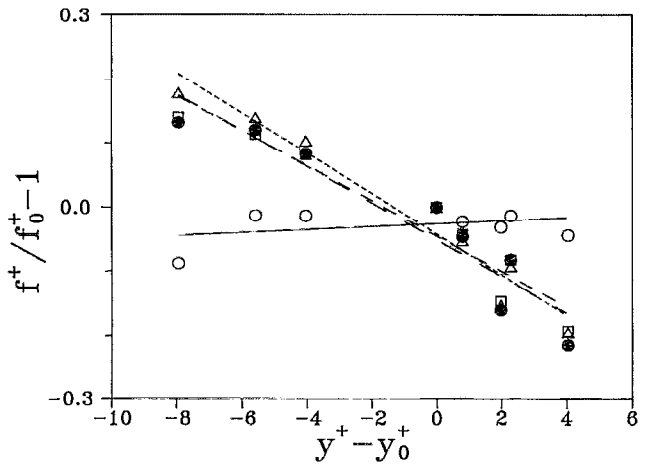

FIG. 6. Normalized maxima for the profiles of the different fluctuation magnitudes, as a function of offset. Symbols are as in Fig. 5. Regression slopes: u', 0.002; v', −0.027; w', −0.031; and $\langle -u'v' \rangle$, −0.028.

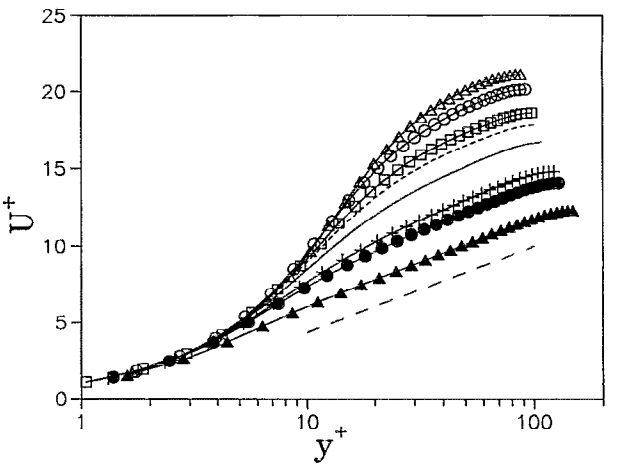

FIG. 8. Mean velocity profiles for controlled channels with different α. Symbols are as in Fig. 3. Dashed straight line corresponds to a von Kármán constant $\kappa=0.41$.

other hand, this trend is consistent with models, like the rapid distortion one, in which the role of the transverse condition is essentially dissipative.

As the transverse flow weakens, so does the skin friction (Fig. 7). This is also consistent with the rapid distortion model. As the streamwise vortices move away from the wall, the normal strain $\partial v/\partial y$ that they induce at the wall becomes weaker, and the viscous boundary layers of the longitudinal velocity become thicker, resulting in a lower wall vorticities. Note that, in the rapid distortion model, the intensity of the maximum u' fluctuation is independent of the position of the vortices, since it is only limited by the alternation of maximum and zero velocities alongside the cores, but that its position moves out with the streamwise vortices. This agrees with the trends in Figs. 5 and 6. A more quantitative discussion of these trends is delayed until the next section.

An interesting observation is that the mean velocity profiles for these highly perturbed channels display a logarithmic region whose slope is consistent with the same von Kármán constant as in the natural case (Fig. 8). Especially interesting is the profile for the free slip case ($\alpha=1$), whose logarithmic region is much longer than would correspond even to its comparatively high Reynolds number, $\mathrm{Re}_\tau \approx 160$. Evidently, the logarithmic law is not particularly influenced by the manipulation of the wall region.

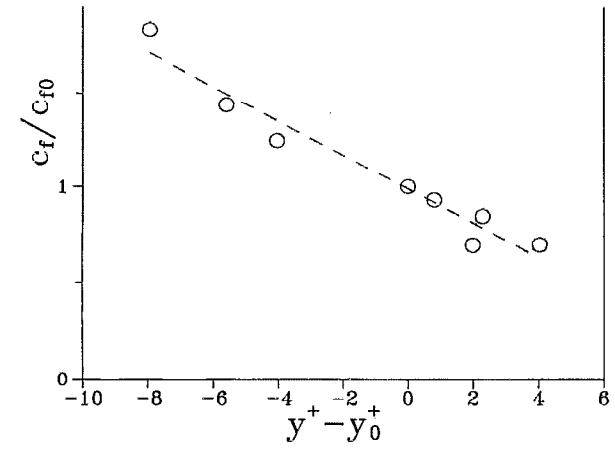

FIG. 7. Variation of the friction coefficient as a function of the vertical offset. Regression slope, −0.09.

V. RIBLETS

The result in Fig. 7 suggests that a similar argument can be used to explain the drag reduction observed in riblet mounted boundary layers.[33] It has been known for some time that the virtual origin for viscous longitudinal flow in those surfaces is lower than that for transverse flow, and the offset between the two origins, the "protrusion height," has been computed for several riblet geometries.[34,35] The observation is that, when the flow is considered at distances from the wall that are large with respect with the protrusion height, it sees both the longitudinal and the transverse zero velocity boundary conditions as applied on a plane, but on a different one for each of them. This is, of course, only true as long as the riblets themselves are small compared to the characteristic length scales of the flow in the vicinity of the wall. The protrusion heights for practical riblets are small, $\Delta y^+=\epsilon=1$–2.

If these conditions are satisfied, the problem looks very similar to the one treated in the previous section, and the behavior of the flow should be qualitatively and even approximately quantitatively similar. It is well known[33] that the optimum performance of riblets of a given shape occurs when their pitch is $s^+\approx 15$. This is consistent with the previous argument, in that this is also the characteristic size of the streamwise vortices. Larger grooves are comparable to the vortices and are not seen as an equivalent boundary condition on a plane. In essence, they are seen as corrugated plates with a strange geometry. It is only below the size of optimum performance that the problem should be equivalent to the one in the previous section. An alter-

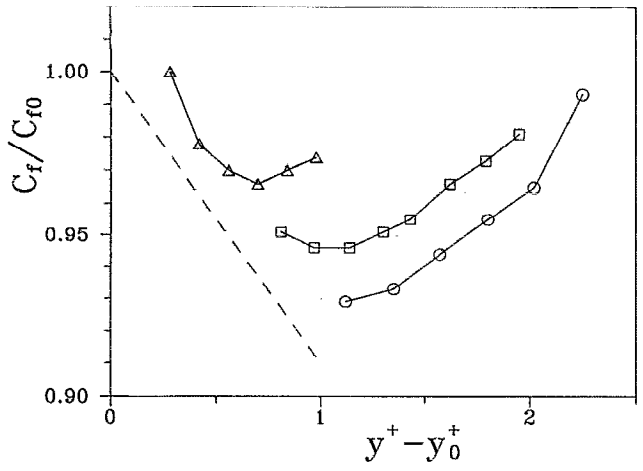

FIG. 9. Drag reduction using riblets as a function of protrusion height. Symbols are different riblets from Ref. 33. ○: triangular, $h/s=0.87$; △: triangular, $h/s=0.45$; □: scalloped, $h/s=0.33$. A dashed line is regression from Fig. 7.

native, and equivalent, argument is that the protrusion height approximation is only valid as long as the inertial terms can be neglected for the flow around the riblets,[35,36] which requires that the Reynolds number based on u_τ and either on the riblet height h or on its pitch should be $O(1)$, and implies that neither s^+ nor h^+ can be too large.

Unfortunately, there are not many experimental measurements in that range of riblet size, but there are enough measurements near optimum performance to interpolate between those points and the zero drag reduction at zero riblet height. We have compiled in Fig. 9 the drag reduction for several riblet shapes in terms of the protrusion heights, and we have compared it with the drag reduction line derived from Fig. 7. The results from the different riblets do not collapse into a single curve because they correspond mostly for sizes larger than the optimum, for which the important parameter is not the boundary offset, but the absolute size with respect to the flow structure. Below the optimum size, however, all the curves can be joined to the point representing the flat plate by curves that are close to each other, and that agree reasonably well with the line obtained from the offset boundary simulations.

First of all, this result has some practical significance; it suggests that the optimum riblet is the one that has the maximum protrusion height, $\Delta y^+=\epsilon_{15}^+$ at $s^+\approx 15$, and it gives an upper bound for the drag reduction to be achieved as $c_f/c_{f0}\approx 1-0.09\,\epsilon_{15}^+$. Perhaps more significantly, it also provides an approximate physical realization for the numerical experiments discussed in the previous section, with results that are close enough to give us some confidence in the correctness of our analysis.

Unfortunately, the numerical resolution of our numerical experiments is not high enough to obtain good structural information, and the little that can be obtained is difficult to compare with that given by previous experimental and numerical studies, which tend to concentrate on the different behaviors of the flow above riblet tips and valleys.[5,37,38] The few results that can be compared directly, such as the upward displacement of the mean velocity profiles, and the constancy of the logarithmic slopes, agree with experimental evidence.[5]

In fact, we can try to apply the estimates in Sec. III to the effect of an offset ϵ between the transverse and longitudinal boundary conditions. Its main effect would be to increase the standoff distance of the vortices above the wall by ϵ, and to substitute ϵ into the right-hand side of Eq. (8). From that equation we can then estimate the derivative of the different quantities with respect to the offset,

$$\frac{1}{\delta_m^+}\frac{d\delta_m^+}{d\epsilon^+}\approx 0.04,$$

$$\frac{1}{R^+}\frac{dR^+}{d\epsilon^+}\approx 0.08, \tag{10}$$

$$\frac{1}{W^+}\frac{dW^+}{d\epsilon^+}\approx 0.12,$$

where δ_m, R, and W are, respectively, the standoff distance of the streamwise vortices above the $w=0$ boundary condition, their radius, and the distance between velocity streaks. The effect on the standoff distance is small, in agreement with the observation that the main effect of the offset is to displace the whole transverse flow by the same amount as the offset. The vortices, however, get thicker and the streaks wider. Observations over riblets show that the width of the streaks grows by 15%–30% for protrusion heights of the order of one to two wall units,[39] which is in good agreement with the derivative in Eq. (10).

An argument that relates the location and intensity of the streamwise to the mean shear was given in Ref. 14. In essence, it assumes that the velocity difference across most of the boundary layer is compressed by the down-draft of the streamwise vortices into viscous wall layers, whose thickness are determined by the viscosity and by the local strain, which is proportional to γ/h^2, where γ is the circulation in a streamwise vortex and $h=R+\delta_m+\epsilon$ is the standoff distance of its center above the $u=0$ wall. The viscous thickness is proportional to $(\nu h^2/\gamma)^{1/2}$, and the skin friction is inversely proportional to it. The circulation in the vortices comes from the one contained in the initial perturbations from which they are formed, which is proportional to the wavelength of the initial instability and therefore to the width of the streak. As a consequence, $\Omega\sim W^{1/2}/h$, and the derivative of the skin friction with respect to the offset can be written as

$$\frac{1}{\Omega}\frac{d\Omega}{d\epsilon^+}=\frac{4}{3}\left(\frac{1}{2W^+}\frac{dW^+}{d\epsilon^+}-\frac{1}{h^+}\frac{dh^+}{d\epsilon^+}\right), \tag{11}$$

where the $\frac{4}{3}$ factor comes from the conversion from absolute quantities to wall units. Using the estimates in Eq. (10), we obtain, after some algebra,

$$\frac{1}{c_f}\frac{dc_f}{d\epsilon^+}=-\frac{1}{R^+}\frac{dR^+}{d\epsilon^+}\approx -0.08,$$

which is in approximate agreement with the value -0.09 obtained from Fig. 7 and with the trend of the efficiency of optimal riblets.

VI. CONCLUSIONS

We have described a simple cycle of events that would result in the maintenance of turbulent flow in the near wall region of a turbulent boundary layer. The two key stages are the advection of the mean shear by the flow in the transverse plane, which leads to the formation of the streaks, and the regeneration of the transverse flow through the shearing and stretching of the lateral instability waves that form in the ω_y regions that separate the streaks. Both processes are essentially inviscid and linear, and are contained in the rapid distortion approximation of shear turbulence. In the first stage kinetic energy flows from the mean shear into the u' fluctuations that constitute the streaks, while, in the second, energy is fed into the cross-flow as some of the vorticity in these fluctuations is tilted into the streamwise direction.

Viscosity act as a limit to the minimum scale that can be achieved by the tilted structures, and it eventually sets the width of the streaks. It also imposes the no-slip boundary condition of u at the wall, and therefore transforms into skin friction the velocity fluctuations present in the streaks. In this way, the viscous sublayer acts like the main seat of dissipation in the boundary layer.

We have shown that this model can be made quantitative, and that it can be used to obtain estimates for the size of the different structures, which agree with experimental observations.

To separate the contributions from different parts of the models, we have presented numerical experiments in which the longitudinal and transverse no-slip boundary conditions are approximately decoupled. We have shown that the variation of the low-order statistics in these experiments agrees with our model, both qualitatively and quantitatively. Finally, we have related the offset boundary conditions to the performance of riblets, and we have shown that our order of magnitude estimates can also provide quantitative information on that problem

The model in this paper can only be considered preliminary, and much work needs to be done before it is checked completely. Some parts of it may turn out to be wrong, but we believe that it is consistent, both with itself and with the experimental observations of the wall region. We have also shown that it is able to predict the response of wall turbulence to some types of perturbations. This is in the end of the mission of simplified models, and the usefulness of this one should be judged on whether it can be made to work in other complicated situations.

ACKNOWLEDGMENTS

Much of this work, including all the control experiments, were carried out at the Center for Turbulence Research, and supported by it. The rest was supported in part by the ESA Hermes program, under contract to Dassault Aviation. I am especially grateful to H. Choi for the free use of his simulation code, and to P. Orlandi for much common work, which is reflected in the model in Sec. II. I also want to acknowledge many useful discussions with P. Moin. Bill Reynolds opened my eyes to the significance of rapid distortion theory.

[1] H. Schlichting, *Boundary Layer Theory*, 6th ed. (McGraw-Hill, New York, 1968), pp. 523–680.
[2] J. D. A. Walker, "Turbulent flow structure near walls," Philos. Trans. R. Soc. London Ser. A **336**, 1 (1991).
[3] D. N. Bushnell and J. N. Hefner (editors), *Viscous Drag Reduction in Boundary Layers* (AIAA, Washington, DC, 1990).
[4] J. Cousteix, "Special course on skin friction drag reduction," AGARD R-786, 1992.
[5] H. Choi, P. Moin, and J. Kim, "Turbulent drag reduction: Studies of feedback control and flow over riblets," Report No. TF-55, Department of Mechanical Engineering, Stanford University, 1992.
[6] H. T. Kim, S. J. Kline, and W. C. Reynolds, "The production of turbulence near a smooth wall in a turbulent boundary layers," J. Fluid Mech. **50**, 133 (1971).
[7] R. F. Blackwelder and H. Eckelmann, "Streamwise vortices associated with the bursting phenomenon," J. Fluid Mech. **94**, 577 (1979).
[8] S. K. Robinson, "Coherent motions in the turbulent boundary layer," Annu. Rev. Fluid Mech. **23**, 601 (1991).
[9] J. Kim, P. Moin, and R. Moser, "Turbulence statistics in fully developed channel flow at low Reynolds number," J. Fluid Mech. **177**, 133 (1987).
[10] P. R. Spalart, "Direct numerical simulation of a turbulent boundary layer up to R_θ=1410," J. Fluid Mech. **187**, 61 (1988).
[11] J. Jiménez and P. Moin, "The minimal flow unit in near wall turbulence," J. Fluid Mech. **225**, 221 (1991).
[12] J-L. Balint, J. M. Wallace, and P. Vukoslavcevic, "The velocity and vorticity vector fields of a turbulent boundary layer. Part 2: Statistical properties," J. Fluid Mech. **228**, 53 (1991).
[13] T. Wei and W. W. Willmarth, "Reynolds number effects on the structure of a turbulent channel flow," J. Fluid Mech. **204**, 57 (1989).
[14] P. Orlandi and J. Jiménez, "On the generation of turbulent wall friction," Phys. Fluids **6**, 634 (1993).
[15] O. Sendstad and P. Moin, "The near wall mechanics of three dimensional turbulent boundary layers," Report No. TF-57, Department of Mechanical Engineering, Stanford University, 1992.
[16] A. E. Perry, S. Henbest, and M. S. Chong, "A theoretical and experimental study of wall turbulence," J. Fluid Mech. **165**, 163 (1986).
[17] P. Orlandi and J. Jiménez, "A model for bursting of near wall vortical structures in boundary layers," in Proceedings of the 8th Symposium on Turbulent Shear Flows, 1991, pp. 28.1.1–28.1.6.
[18] J. Jiménez and P. Orlandi, "The roll-up of a vortex layer near a wall," J. Fluid Mech. **248**, 297 (1993).
[19] T. L. Doligalski and J. D. A. Walker, "The boundary layer induced by a convected two-dimensional vortex," J. Fluid. Mech. **139**, 1 (1984).
[20] C. R. Smith, J. D. A. Walker, A. H. Haidari, and U. Sobrun, "On the dynamics of near-wall turbulence," Philos. Trans. R. Soc. London Ser. A **336**, 131 (1991).
[21] M. T. Landahl, "On sublayer streaks," J. Fluid Mech. **212**, 593 (1991).
[22] A. V. Johansson, P. H. Alfredsson, and J. Kim, "Evolution and dynamics of shear-layer structures in near-wall turbulence," J. Fluid Mech. **224**, 579 (1991).
[23] J. D. Swearingen and R. F. Blackwelder, "The growth and breakdown of streamwise vortices in the presence of a wall," J. Fluid Mech. **182**, 255 (1987).
[24] A. A. Townsend, "Entrainment and the structure of turbulent flow," J. Fluid Mech. **41**, 13 (1970).
[25] M. R. Maxey, "Distortion of turbulence in flows with parallel streamlines," J. Fluid Mech. **124**, 261 (1982).
[26] M. J. Lee, J. Kim, and P. Moin, "Structure of turbulence at high shear rate," J. Fluid Mech. **216**, 561 (1990).
[27] M. M. Rogers and P. Moin, "The structure of the vorticity field in homogenous turbulent flows," J. Fluid Mech. **176**, 33 (1987).
[28] C. R. Smith and S. P. Metzler, "The characteristics of low speed streaks in the near wall region of a turbulent boundary layer," J. Fluid Mech. **129**, 27 (1983).
[29] J. Jiménez, "On small scale vortices in turbulent flows," in *New Approaches and Concepts in Turbulence*, edited by T. Dracos and A. Tsinober (Birkäuser, Basel, 1993), pp. 95–110; also see Phys. Fluids A **4**, 652 (1992).

[30]P. G. Drazin and W. H. Reid, *Hydrodynamic Instability* (Cambridge U.P., Cambridge, 1981), pp. 231–239.
[31]P. Orlandi, "Vortex dipole rebound from a wall," Phys. Fluids A **2**, 1429 (1990).
[32]J. Jiménez, "Wall friction and the structure of near-wall turbulence," in *Proceedings of the 11th Australasian Fluid Mechanics Conference*, edited by M. R. Davis and G. J. Walker (University of Tasmania, Hobart, 1992), pp. 813–816.
[33]M. J. Walsh and A. M. Lindemann, "Optimization and application of riblets for turbulent drag reduction," AIAA Paper No. 84-0347, 1984.
[34]D. W. Bechert, M. Bartenwerfer, and G. Hoppe, "Turbulent drag reduction by nonplanar surfaces—A survey on the research at TU/DLR Berlin," in *Structure of Turbulence and Drag Reduction*, edited by A. Gyr (Springer-Verlag, Berlin, 1989), pp. 525–543.
[35]P. Luchini, F. Manzo, and A. Pozzi, "Resistance of a grooved surface to parallel flow and cross-flow," J. Fluid Mech. **228**, 87 (1991).
[36]D. W. Bechert and M. Bartenwerfer, "The viscous flow on surfaces with longitudinal ribs," J. Fluid Mech. **206**, 105 (1989).
[37]K-S. Choi, "Near wall structure of a turbulent boundary layer with riblets," J. Fluid Mech. **208**, 417 (1989).
[38]P. Vukoslavcevic, J. M. Wallace, and J-L. Balint, "Viscous drag reduction using streamwise aligned riblets," AIAA J. **30**, 1119 (1992).
[39]M. J. Walsh, "Riblets," in *Viscous Drag Reduction in Boundary Layers*, edited by D. M. Bushnell and J. N. Hefner (AIAA, Washington, DC, 1990), pp. 203–261.
[40]R. Corral and J. Jiménez, "Direct numerical simulation of the subcritical boundary layer," Technical Note ETSIA/MF-921, School of Aeronautics, Madrid, 1992.
[41]R. Corral and J. Jiménez, "Fourier–Tchebichev methods for the incompressible Navier Stokes equations in infinite domains," submitted to J. Comput. Phys.